Supplementary Tables and Figures

Table S1. Expression analysis of known YAP/TAZ/TEAD target genes in human ADPKD cysts, minimally cystic tissues (MCT) and normal kidneys (KIDNEY).
The Excel file shows the raw data for the expression of a previously reported set of 379 YAP/TAZ/TEAD direct target genes and the relative fold change of expression in human ADPKD cysts relative to minimally cystic tissues or normal kidneys.

Table S2. A summary of YAP/TAZ/TEAD direct target genes with altered expression in human ADPKD cysts versus minimally cystic tissues (MCT).
The Excel file shows the raw data for the expression of 203 YAP/TAZ/TEAD direct target genes and the relative fold change of expression in human ADPKD cysts relative to minimally cystic tissues.

Table S3. A summary of animals used for phenotypic analyses in this study.
The Excel file shows the genotype, age, gender, treatment, kidney weight, body weight, and the ratio of kidney over body weight for each animal analyzed.

Table S4. PCR Primers and site-directed mutagenesis

Real time PCR primer	Sequence
c-Myc forward	CCTTTGGGCGTTGGAAACC
c-Myc reverse	CGTCGCAGATGAAATAGGG
Cyr61 forward	GCTCAGTCAGAAGGCAGACC
Cyr61 reverse	GTTCTTGGGGACACAGAGGA
Ctgf forward	AGTGTGCACTGCCAAAGATG
Ctgf reverse	CCAGGCAAGTGCATTGGTAT
Col12A1 forward	AAGTTGACCCACCTTCCGAC
Col12A1 reverse	GGTCCACTGTTATTCTGTAACCC
Amotl2 forward	AGGGACAATGAGCGATTGCAG
Amotl2 reverse	CCTCACGCTTGGAAGAGGT
Axl forward	ATGGCCGACATTGCCAGTG
Axl reverse	CGGTAGTAATCCCCGTTGTAGA
Gapdh forward	CCCAATGTGTCCGTCGTGGAT
Gapdh reverse	TGTAGCCCAAGATGCCCTTCAG
ChIP PCR primer	**Sequence**
Site 1 forward	TGAGGTTCTGGGCACTGTGA
Site 1 reverse	CTTTCCAGAAGATCCTAGTC
Site 2 forward	TGTAGGTAGAGTGGCACAGG
Site 2 reverse	GGACAGGAAAGCCACAAGTT
Site 3 forward	GATTGGTGGCTCTTGGTGTT
Site 3 reverse	GCCACTGAGTTTGCAATTTAGG
Site 4 forward	GGGGTCGTTCTGGAAAGAAT
Site 4 reverse	AGCAACTCACTGCCACGTAT
Site 5 forward	CCATTCCTGTGCTTTTGACA
Site 5 reverse	GGTTTTTCCCTTCCCCTTTC
Site 6 forward	TTGGGACAGGGATGTGACCG
Site 6 reverse	CTCAGATCACGACTCACCGC
Enhancer PCR primers	**Sequence**
Pro1 forward	GGGCCGACTTGTTCATTCTA
Pro1 reverse	AAGGACAGGAAAGCCACAAG
Pro2 forward	GATTGGTGGCTCTTGGTGTT
Pro2 reverse	TGCAGGAAAAACGATGTCTG
Int1 forward	CTGGTGGTCTTTCCCTGTGT
Int1 reverse	GGGAGGGGGTGTCAAATAAT

	Original sequence	Mutagenesis sequence
Site 1	GTAAGAGGGAATGTACTCTC	GTAAGAGGGATCCTACTCTC
Site 2	AACAAGAACATTCCAATCAC	AACAAGAACATGTCAATCAC
Site 5	CTTTCTTCCATTCCTGTGCT	CTTTCTTCCATGGCTGTGCT
Site 6	GAATCCTCCATTCCTACTTG	GAATCCTCCATGGCTACTTG

Figure S1. Activity of the *AhCre* driver in the kidney.

(A) β-galactosidase staining in P12 *Rosa26LacZ*/+ kidneys. Scale bars, 100 μm.

(B) β-galactosidase staining in P12 *AhCre;R26RLacZ*/+ kidneys without β-NF induction. Scale bars, 100 μm.

(C) β-galactosidase staining in P12 *AhCre;R26RLacZ*/+ kidneys after daily β-NF injections from P8 to P11. Scale bar, 100 μm. A higher magnification view of kidney section showing LacZ-positive cells is shown to the right.

(D) Morphology of the kidneys in control ($Pkd1^{flox/flox}$) and *Pkd1* mutant ($AhCre;Pkd1^{flox/flox}$) mice 3 weeks after P8-P11 β-NF injections.

(E) H&E staining of *Pkd1* mutant kidneys 3 weeks after P8-P11 β-NF injections. Scale bar, 1 mm. A higher magnification view of kidney section is shown to the right. The arrow marks kidney cysts, while the arrowhead indicates glomerular dilation.

(F) Lectin *Lotus tetragonolobus* (LTL), Tamm-Horsfall protein (THP) and lectin *Dolichos biflorus* (DBA) staining in *Pkd1* mutant kidneys 3 weeks after β-NF injections. LTL, THP and DBA are segment-specific markers: LTL for the proximal tubule, THP for the thick ascending limb and distal convoluted tubule, and DBA for the collecting duct. Arrows indicate cysts in the proximal tubule (LTL-positive), the thick ascending limb and distal convoluted tubule (THP-positive) and the colleting duct (DBA-positive). Scale bar, 100 μm.

Figure S1

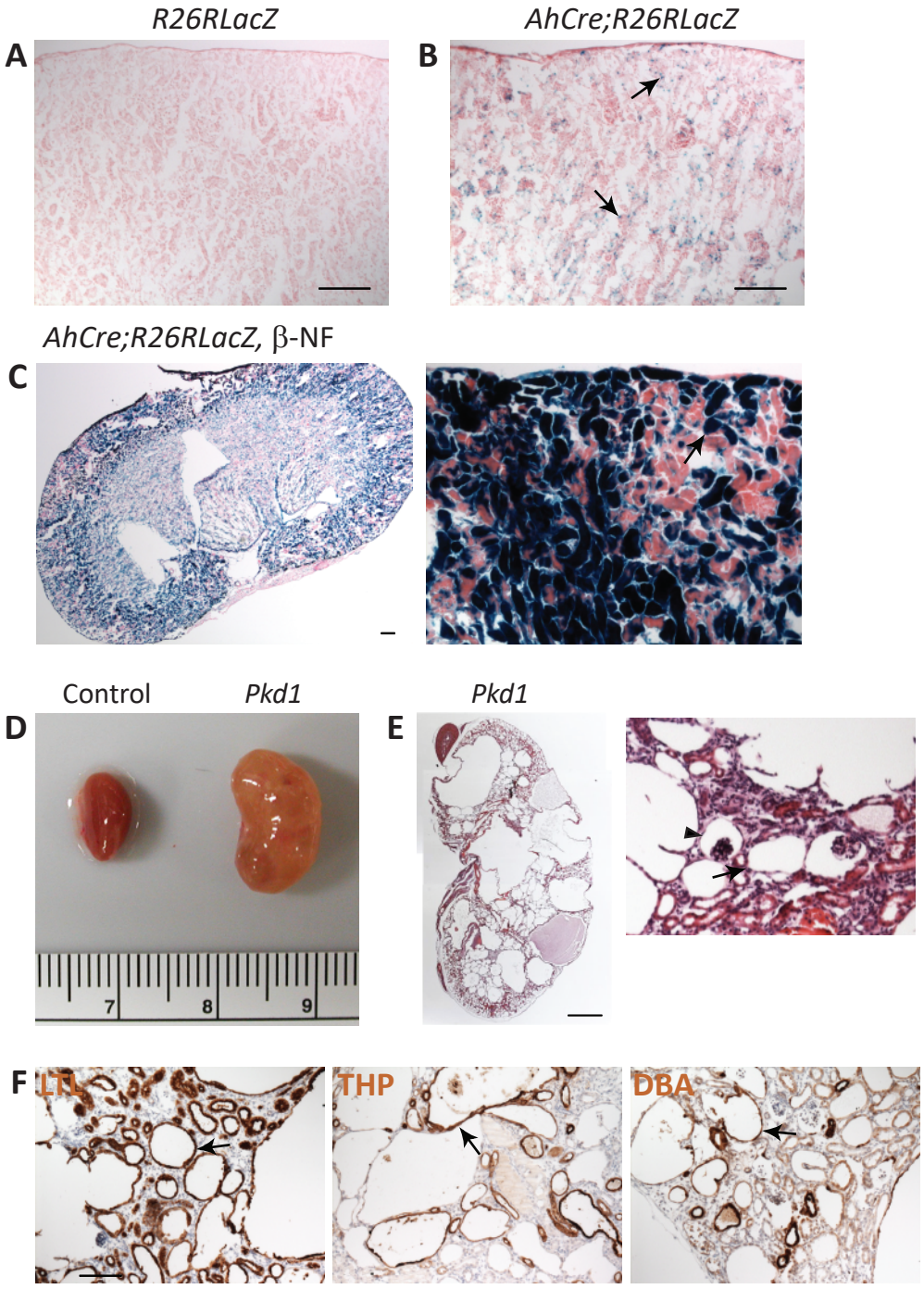
R26RLacZ
AhCre;R26RLacZ
A
B
AhCre;R26RLacZ, β-NF
C
Control
Pkd1
Pkd1
D
E
F
LTL
THP
DBA

Figure S2. YAP activation in renal tubular epithelium leads to tubule dilation in the kidney.

(A-B) Double staining of YAP and LTL (A) and YAP and BDA (B) showing overexpressed YAP protein in the proximal tubule (LTL-positive) and the collecting duct (DBA-positive) in the kidney tubular epithelium (arrows) after doxycycline treatment of *Pax8-rtTA;pTRE2-Yap* double transgenic mice for 2 days. Scale bar, 100 μm. A higher magnification view of kidney section is shown to the right.

(C-E) LTL (C), THP (D) and DBA (E) staining showing progression of kidney tubule dilation in the proximal tubule (LTL-positive) and the thick ascending limb and distal convoluted tubule (THP-positive), but not in the colleting duct (DBA-positive), upon YAP induction in the double transgenic mice. Tubule dilation began at 4 days after doxycycline induction and progressed to more severe phenotypes by 8 days. Arrows mark representative dilations, while arrowhead indicates a glomerular dilation. Scale bar, 100 μm.

Figure S2

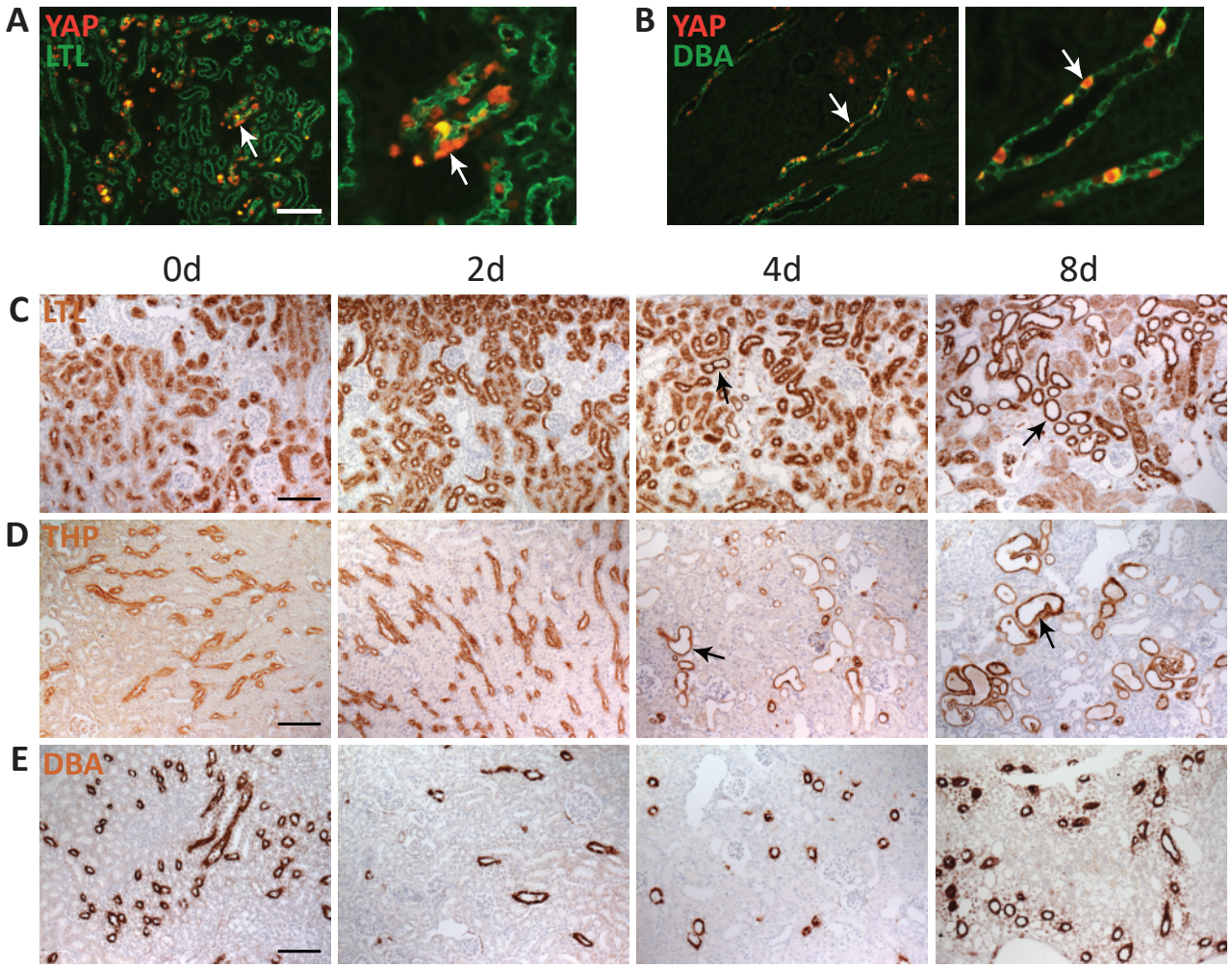

Figure S3. Suppression of hyperproliferation and tubule dilation in *Sav1* mutant kidneys by inactivation of YAP.

Ki67 (A), H&E (B), LTL (C), THP (D) and DBA (E) staining in control, *Sav1* mutant (*AhCre;Sav1*$^{flox/flox}$), *Sav1;Yap* double mutant (*AhCre;Sav1*$^{flox/flox}$*;Yap*$^{flox/flox}$) and *Yap* mutant (*AhCre;Yap*$^{flox/flox}$) kidneys 3 months after P8-P11 β-NF injections. Arrows indicate proliferating cells (A) and dilations (B-D) in the kidney tubular epithelium, while arrowhead indicates a glomerular dilation. Note the dilations in the proximal tubule (LTL-positive) and the thick ascending limb and distal convoluted tubule (THP-positive), but not in the colleting duct (DBA-positive) in *Sav1* mutant kidney tubular epithelium. Scale bars, 100 μm.

Figure S3

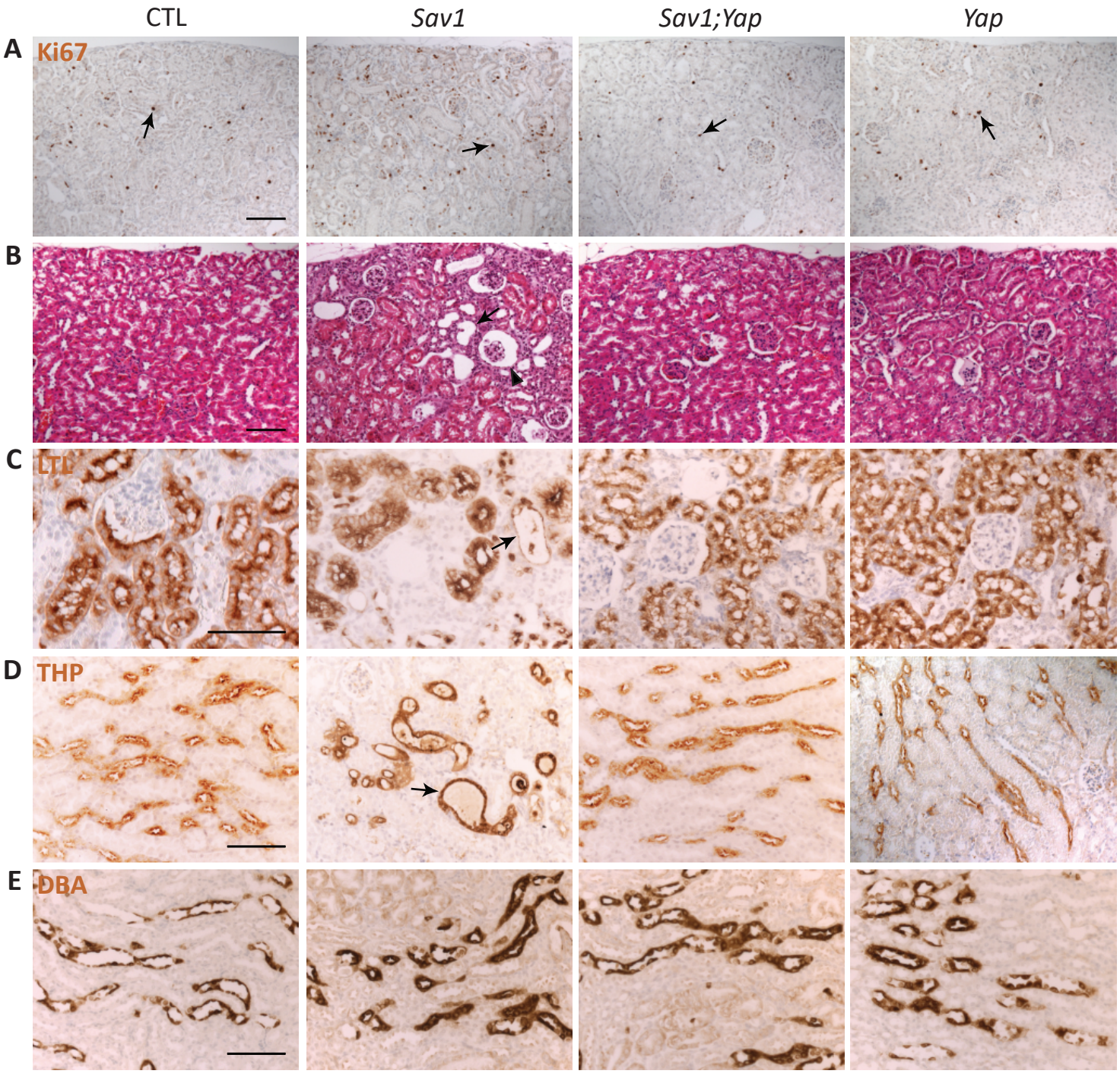

Figure S4. *Taz* mutant mice does not show kidney phenotypes.

(A) LTL, THP and DBA staining in the kidneys of 1-month-old *AhCre;Pkd1*$^{flox/flox}$ mice without β-NF induction. Arrows indicate cysts in the proximal tubule (LTL-positive), the thick ascending limb and distal convoluted tubule (THP-positive) and the colleting duct (DBA-positive). Scale bar, 100 μm.

(B) H&E staining in the kidney of 3-month-old *Taz* mutant (*AhCre;Taz*$^{flox/flox}$) kidneys without β-NF induction. Note the normal histology of *Taz* mutant kidney.

Figure S4

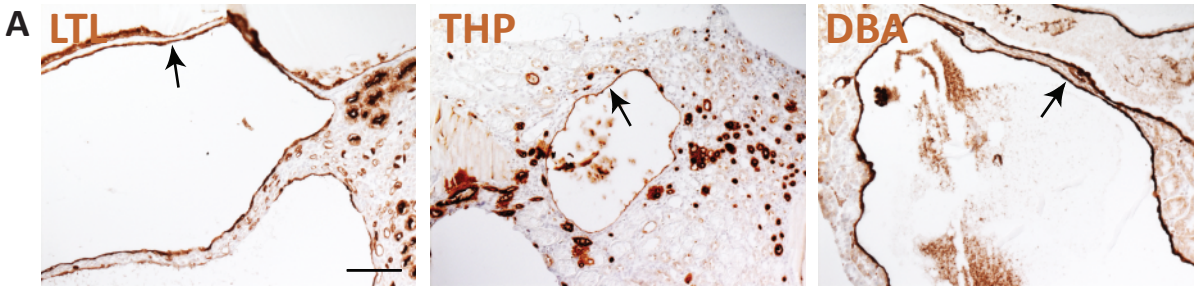

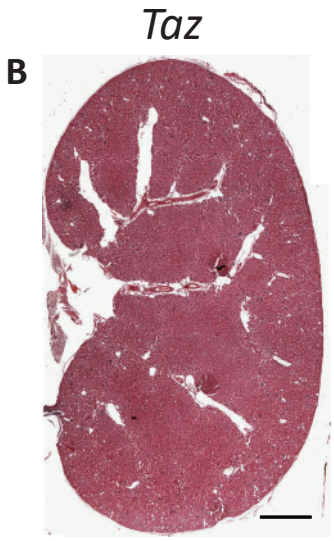

Figure S5. *c-Myc* is a target of YAP in kidney tubular epithelium.

(A) c-Myc staining in kidney tubular epithelium of control and *Pax8-rtTA;pTRE2-Yap* mice 8 days after doxycycline treatment. Note the elevated c-Myc staining after YAP induction. Scale bars, 100 μm.

(B) Loss of YAP suppressed the upregulated c-Myc protein levels in tubular epithelium of *Sav1* mutant (*AhCre;Sav1*$^{flox/flox}$) kidneys 3 months after P8-P11 β-NF injections. Note the elevated c-Myc staining in *Sav1* mutant kidneys, and the normal c-Myc staining in control, *Sav1;Yap* double mutant (*AhCre;Sav1*$^{flox/flox}$*;Yap*$^{flox/flox}$) and *Yap* mutant (*AhCre;Yap*$^{flox/flox}$) kidneys. Scale bars, 100 μm.

(C) Loss of YAP and TAZ suppressed the c-Myc protein levels in kidney cysts of *Pkd1* mutant (*AhCre;Pkd1*$^{flox/flox}$). Note the absence of c-Myc nuclear staining in *Pkd1;YAP;TAZ* triple mutant kidney cysts. Scale bars, 100 μm.

Figure S5

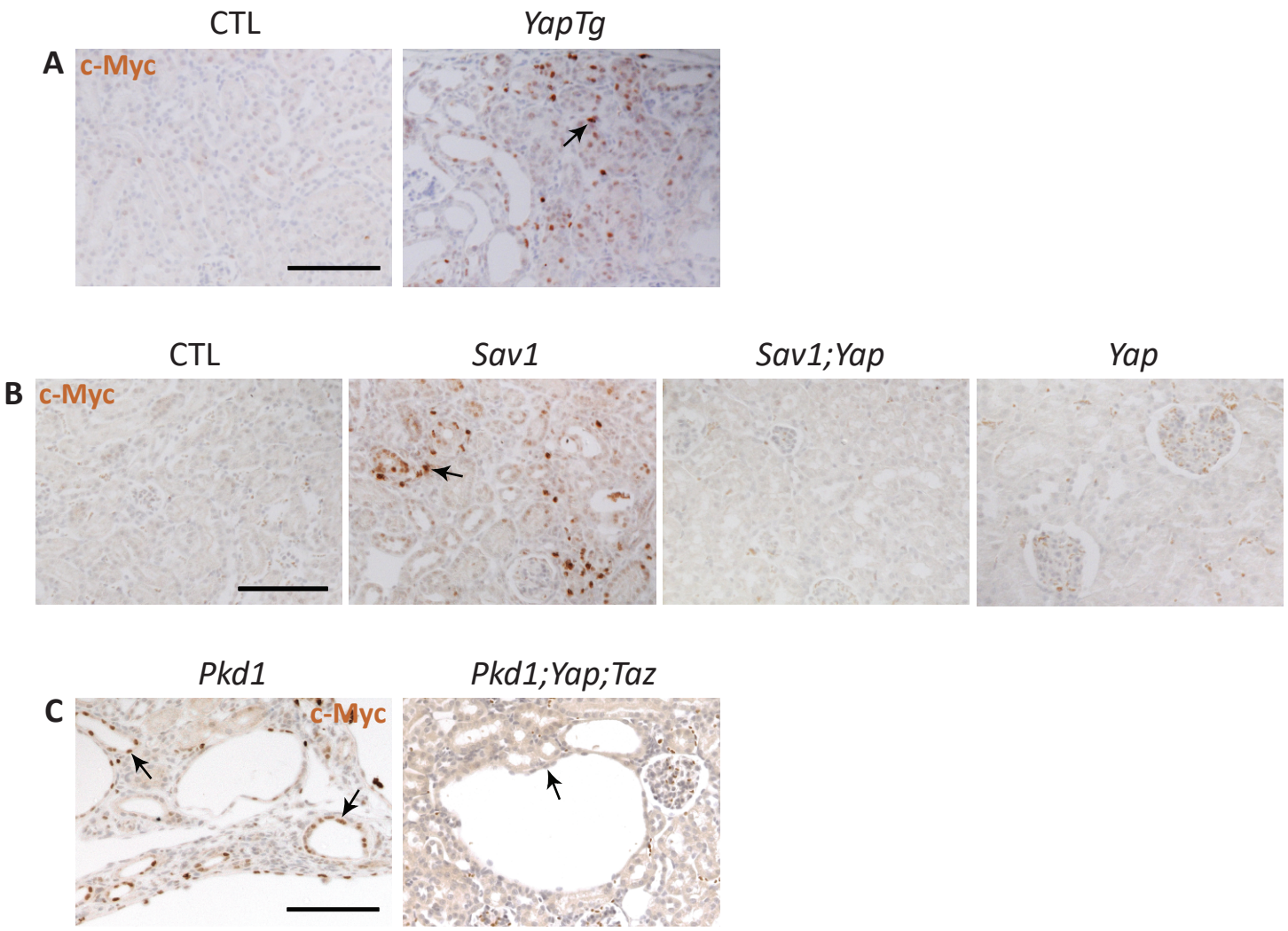
CTL
YapTg
A
c-Myc
CTL
Sav1
Sav1;Yap
Yap
B
c-Myc
Pkd1
Pkd1;Yap;Taz
C
c-Myc

Figure S6. Suppression of tubule dilation in *Sav1* mutant kidneys by inactivation of c-Myc.

LTL (A), THP (B) and DBA (C) staining in control, *Sav1* mutant (*AhCre;Sav1*$^{flox/flox}$), *Sav1;c-Myc* double mutant (*AhCre;Sav1*$^{flox/flox}$*;c-Myc*$^{flox/flox}$) and *c-Myc* mutant (*AhCre;c-Myc*$^{flox/flox}$) kidneys 3 months after P8-P11 β-NF injections. Arrows indicate dilations in the kidney tubular epithelium. Scale bar, 100 μm.

Figure S6

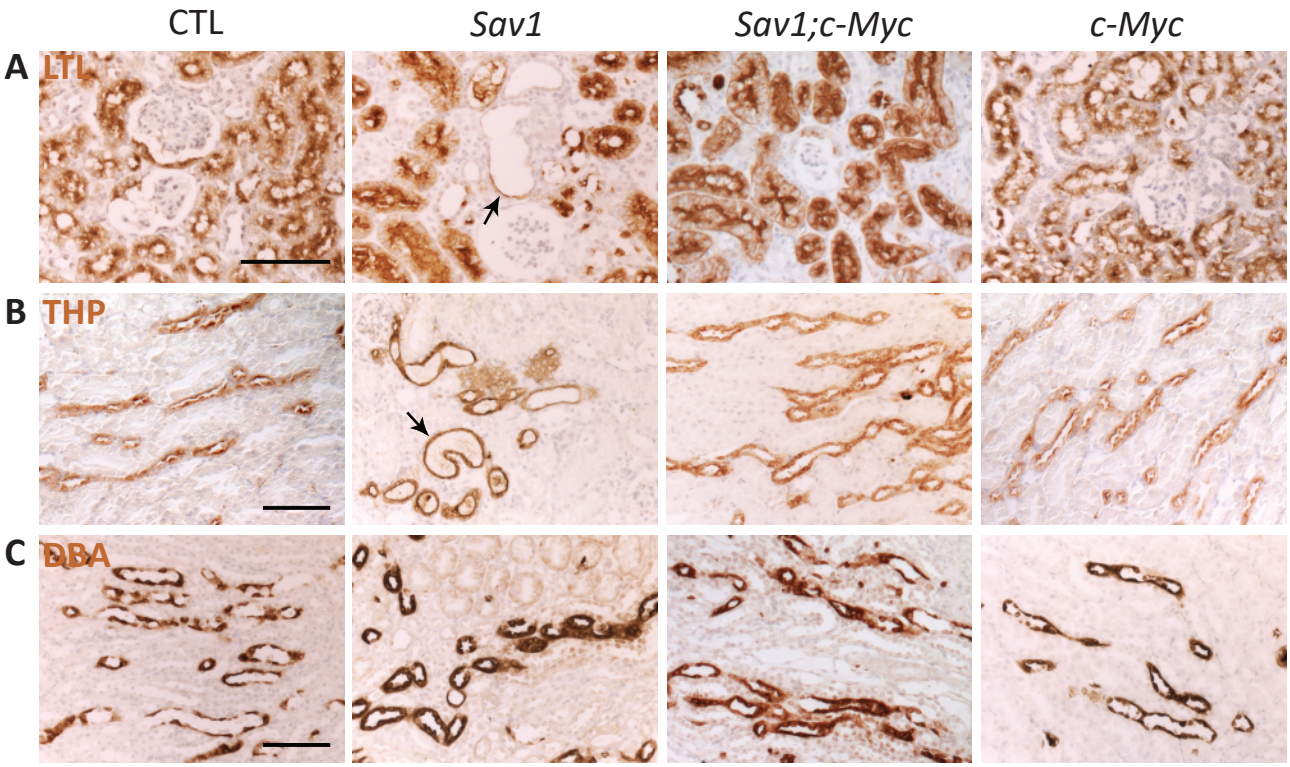

Figure S7. Suppression of tumorigenesis in *Sav1* mutant livers by inactivation of *c-Myc*.

(A) Quantification of liver weight (LW) over body weight (BW) in control (*Sav1*$^{flox/flox}$) (3 mon, n=6; 12 mon, n=4), *Sav1* mutant (*AhCre;Sav1*$^{flox/flox}$) (3 mon, n=4; 12 mon, n=5), *Sav1;c-Myc* double mutant (*AhCre;Sav1*$^{flox/flox}$*;c-Myc*$^{flox/flox}$) (3 mon, n=4; 12 mon, n=4) and *c-Myc* mutant (*AhCre;c-Myc*$^{flox/flox}$) (3 mon, n=4; 12 mon, n=4) mice 3 and 12 months after P8-P11 β-NF injections. Data are mean ± SD. (*) $P<0.01$, *t*-test.

(B) Ki67 staining in control, *Sav1* mutant, *Sav1;c-Myc* double mutant and *c-Myc* mutant livers 3 months after P8-P11 β-NF injections. Arrows indicate proliferating cells in kidney tubular epithelium. Scale bar, 100 μm.

(C) Quantification of Ki67-positive cells in (B). Data are mean ± SD. n = 3. (*) $P<0.01$, *t*-test.

(D-E) Morphology (D) and H&E staining (E) of control, *Sav1* mutant, *Sav1;c-Myc* double mutant and *c-Myc* mutant livers 12 months after P8-P11 β-NF injections. Note the large tumors (D) and a disorganized parenchyma with the characteristics of hepatocellular carcinomas by histological analysis (E) in *Sav1* mutant livers and the complete suppression of tumor formation by loss of c-Myc. Scale bar, 100 μm.

Figure S7

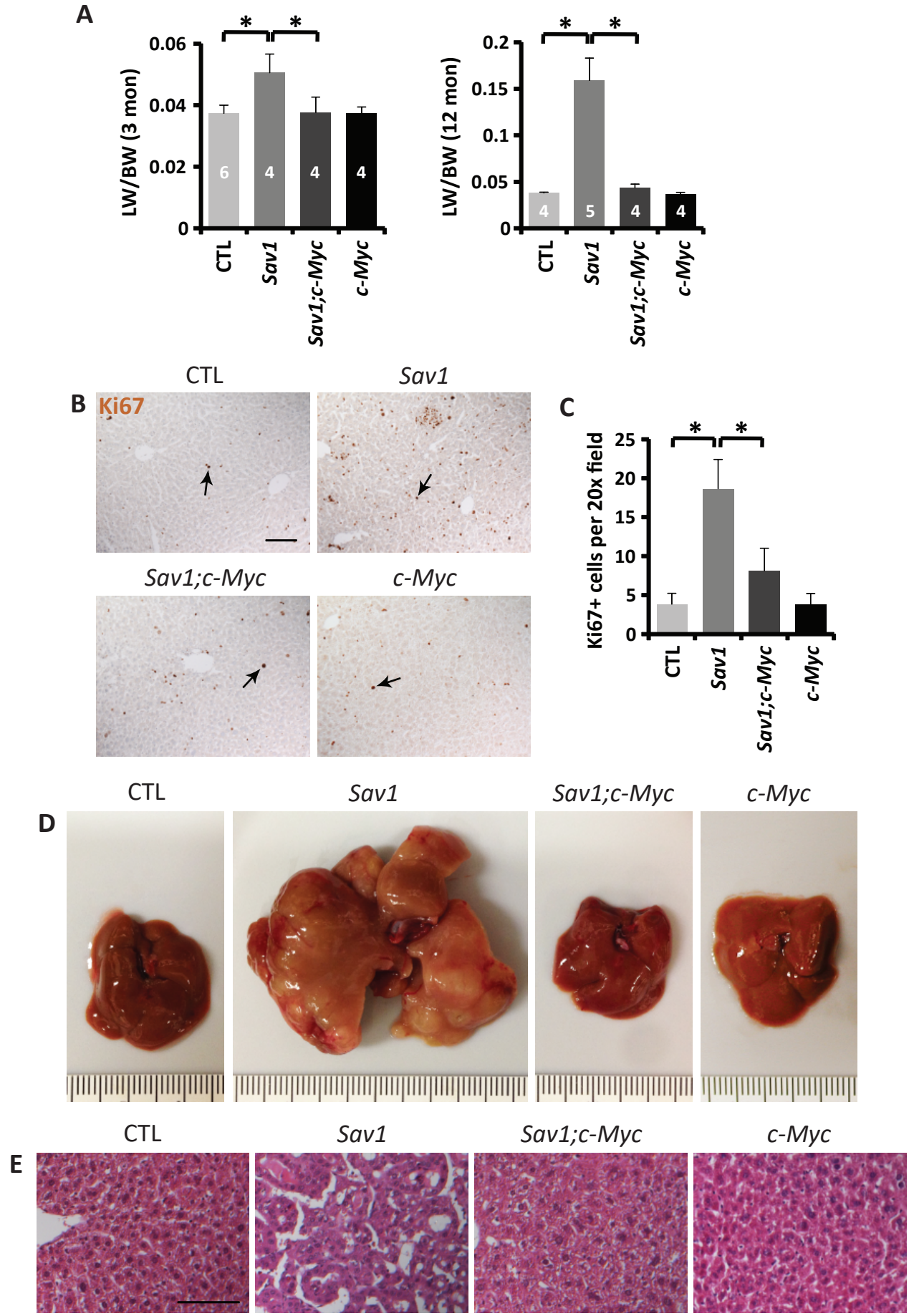
A
LW/BW (3 mon)
0.06
0.04
0.02
0
6
4
4
4
CTL
Sav1
Sav1;c-Myc
c-Myc
LW/BW (12 mon)
0.2
0.15
0.1
0.05
0
4
5
4
4
B
CTL
Sav1
Ki67
Sav1;c-Myc
c-Myc
C
Ki67+ cells per 20x field
25
20
15
10
5
0
D
CTL
Sav1
Sav1;c-Myc
c-Myc
E
CTL
Sav1
Sav1;c-Myc
c-Myc

Figure S8. Development of tubular and cystic structures in 3D-cultured mIMCD3 cells and the effect of ROCK inhibitors on *Pkd1* mutant mIMCD3 cells.

(A) Development of tubular structures in 3D-cultured mIMCD3 cells. Tubule-forming cells initially grew into cell cords without a lumen. Lumen was first seen in cell cords after 5-6 days of culture. Red, phalloidin staining. Blue, DAPI staining. Scale bars, 100 μm.

(B) Development of cystic structures in 3D-cultured mIMCD3 cells. Cyst-forming cells initially grew into cell aggregates without a lumen. Lumen was first seen after 3-4 days of culture in cell aggregates containing about 8 cells. Red, phalloidin staining. Blue, DAPI staining. Scale bars, 100 μm.

(C) Quantification of the percentage of cords/tubules versus cysts in *Pkd1* mutant mIMCD3 cells (clone #1) in 3D culture for 6 days in the presence of the indicated ROCK inhibitors. Note that these ROCK inhibitors induced tubulogenesis in *Pkd1* mutant mIMCD3 cells in a dosage-dependent manner. Co, cord; Tu, tubule. Data are mean ± SD. n=3. (*) $P<0.01$, *t*-test.

(D) Kinase target(s) of the five chemicals that induced tubulogenesis in 3D-cultured *Pkd1* mutant mIMCD3 cells. Information is taken from the commercial supplier of the kinase inhibitor library (https://www.caymanchem.com).

Figure S8

A

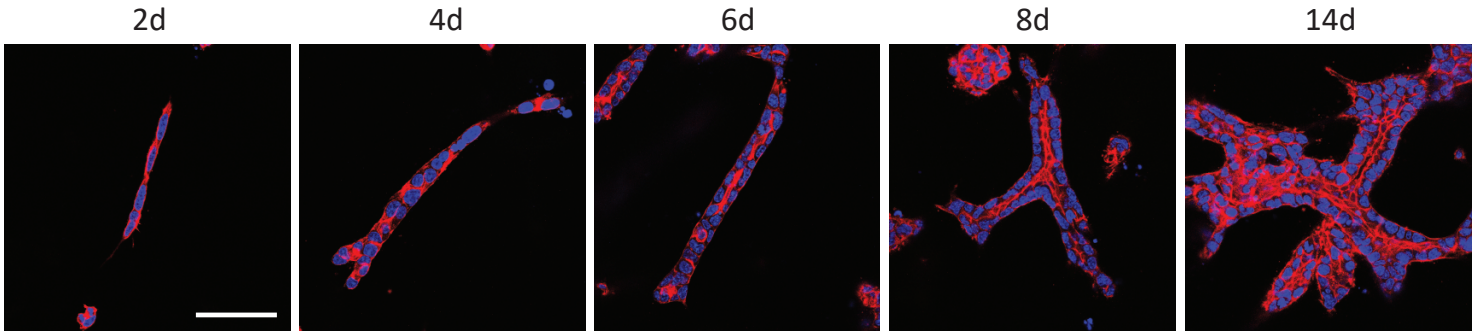

B

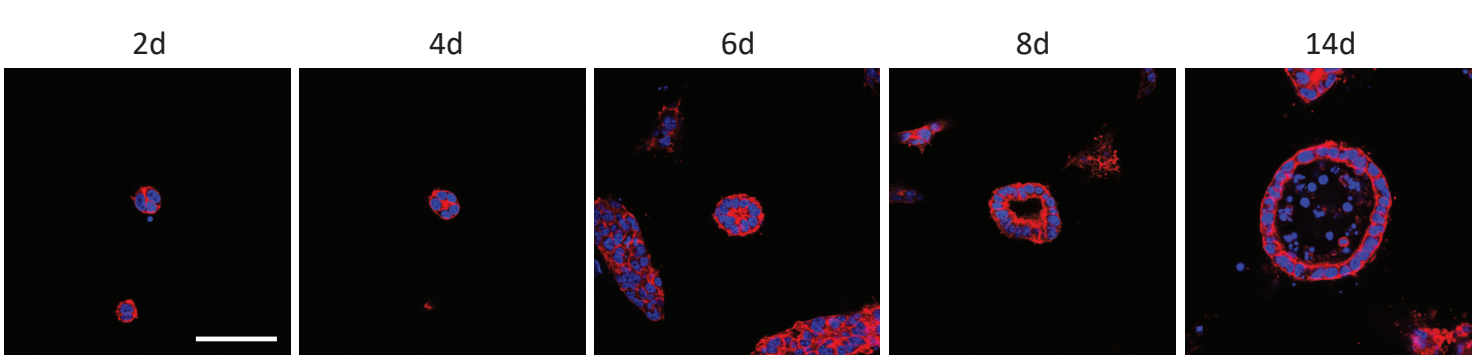

C

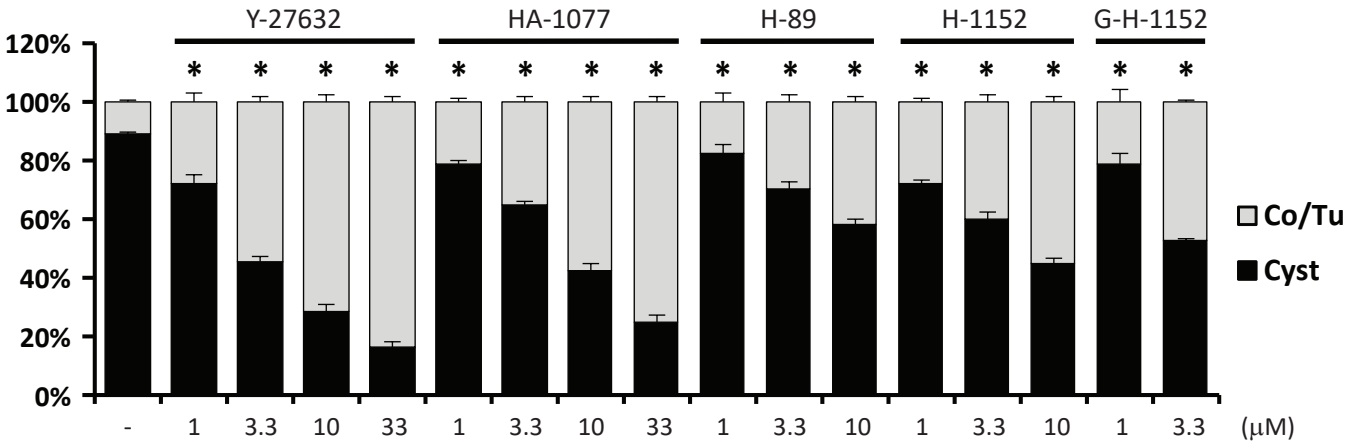

D

Inhibitors	Kinase target
Y-27632	**ROCK**
HA-1077	**ROCK**, PRK2, MSK1, MAPKAP-K1b
H-89	S6K1, MSK1, PKA, **ROCK**, PKBα and MAPKAP-K1b
(S)-H-1152	**ROCK**
(S)-Glycyl-H-1152	**ROCK**

Figure S9. Generation of *Pkd1*, *RhoA* and *Larg* knockout mIMCD3 cells by CRISPR/Cas9.

(A-C) Schematic representation of the mouse *Pkd1*, *RhoA* and *Larg* locus showing the sequence of small guide RNA (sgRNA, underlined) and protospacer adjacent motif (PAM, red color font). DNA sequencing of the induced mutations at the corresponding locus is also shown. When different mutations were induced in the same gene on the homologous chromosomes, both alleles (A & B) are shown.

(A) Characterization of two independent clones of *Pkd1* mutant mIMCD3 cells. Clone #1 was used for subsequent generation of *Pkd1*;*RhoA* or *Pkd1*;*Larg* double mutant cells.

(B) Characterization of two independent clones of *RhoA* mutant and two independent clones of *Pkd1*;*RhoA* double mutant mIMCD3 cells. Also shown is western blotting analysis of cell extracts confirming RhoA inactivation.

(C) Characterization of two independent clones of *Larg* mutant and two independent clones of *Pkd1*;*Larg* double mutant mIMCD3 cells. Also shown is western blotting analysis of cell extracts confirming LARG inactivation.

Figure S9

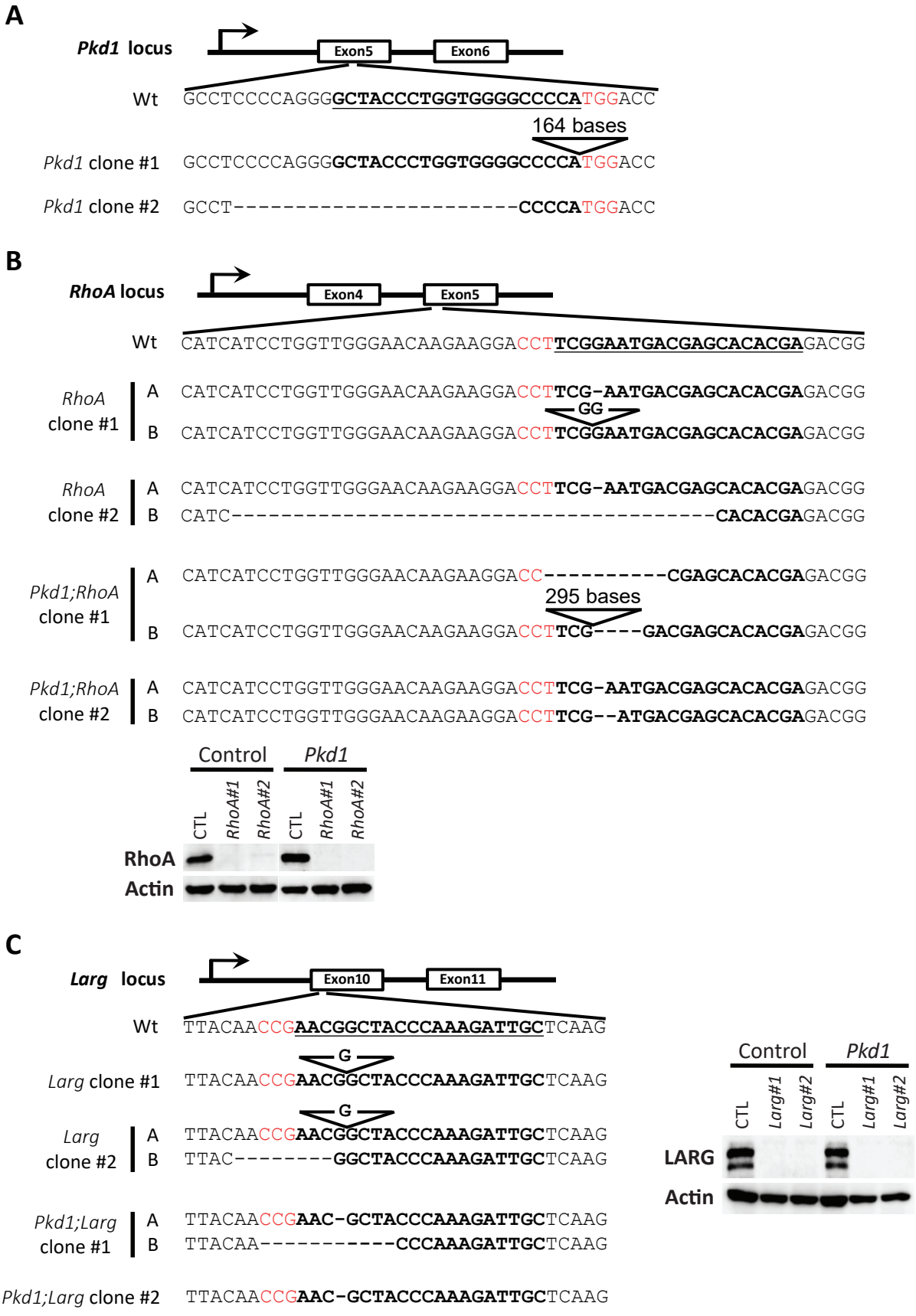
A
Pkd1 locus
Exon5
Exon6
Wt
GCCTCCCCAGGGGCTACCCTGGTGGGGCCCCATGGACC
164 bases
Pkd1 clone #1
GCCTCCCCAGGGGCTACCCTGGTGGGGCCCCATGGACC
Pkd1 clone #2
GCCT----------CCCCATGGACC
B
RhoA locus
Exon4
Exon5
Wt
CATCATCCTGGTTGGGAACAAGAAGGACCTTCGGAATGACGAGCACACGAGACGG
RhoA clone #1
A
CATCATCCTGGTTGGGAACAAGAAGGACCTTCG-AATGACGAGCACACGAGACGG
GG
B
CATCATCCTGGTTGGGAACAAGAAGGACCTTCGGAATGACGAGCACACGAGACGG
RhoA clone #2
A
CATCATCCTGGTTGGGAACAAGAAGGACCTTCG-AATGACGAGCACACGAGACGG
B
CATC----------CACACGAGACGG
Pkd1;RhoA clone #1
A
CATCATCCTGGTTGGGAACAAGAAGGACC----------CGAGCACACGAGACGG
295 bases
B
CATCATCCTGGTTGGGAACAAGAAGGACCTTCG----GACGAGCACACGAGACGG
Pkd1;RhoA clone #2
A
CATCATCCTGGTTGGGAACAAGAAGGACCTTCG-AATGACGAGCACACGAGACGG
B
CATCATCCTGGTTGGGAACAAGAAGGACCTTCG--ATGACGAGCACACGAGACGG
Control
Pkd1
CTL
RhoA#1
RhoA#2
CTL
RhoA#1
RhoA#2
RhoA
Actin
C
Larg locus
Exon10
Exon11
Wt
TTACAACCGAACGGCTACCCAAAGATTGCTCAAG
G
Larg clone #1
TTACAACCGAACGGCTACCCAAAGATTGCTCAAG
G
Larg clone #2
A
TTACAACCGAACGGCTACCCAAAGATTGCTCAAG
B
TTAC--------GGCTACCCAAAGATTGCTCAAG
Pkd1;Larg clone #1
A
TTACAACCGAAC-GCTACCCAAAGATTGCTCAAG
B
TTACAA----------CCCAAAGATTGCTCAAG
Pkd1;Larg clone #2
TTACAACCGAAC-GCTACCCAAAGATTGCTCAAG
Control
Pkd1
CTL
Larg#1
Larg#2
CTL
Larg#1
Larg#2
LARG
Actin

Figure S10. The ROCK inhibitor Y-27632 suppresses YAP activity.

(A) Western blot showing decreased phosphorylation of MLC and increased phosphorylation of Lats1/2 and YAP in mIMCD3 cells after 2 hours treatment with 50 μM Y-27632.

(B) Downregulation of YAP transcriptional target genes in mIMCD3 cells after 2 hours treatment with 50 μM Y-27632. Data are mean ± SD. n = 3. (*) $P<0.01$, *t*-test.

Figure S10

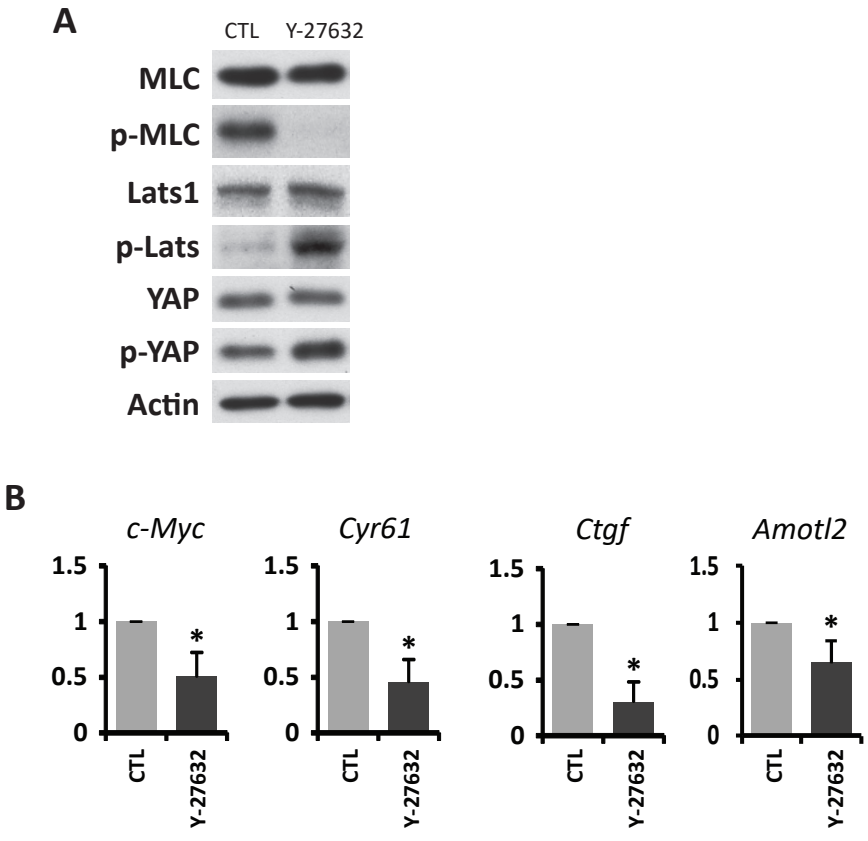
A
CTL
Y-27632
MLC
p-MLC
Lats1
p-Lats
YAP
p-YAP
Actin
B
c-Myc
Cyr61
Ctgf
Amotl2
1.5
1
0.5
0
*
CTL
Y-27632

Figure S11. Subcellular localization of several RhoGEFs in control and *Pkd1* mutant mouse kidneys.

Staining of p115RhoGEF, AKAP13, p63RhoGEF, GEF-H1 and TRIO in control and *Pkd1* mutant kidneys as described in **Figure 1D**. Note the invariable cytoplasmic staining of all these RhoGEFs in control tubular epithelium and *Pkd1* mutant kidney cysts. Scale bar, 100 μm.

Figure S11